THERMAL EVOLUTION OF THE MOON

M. NAFI TOKSŐZ, SEAN C. SOLOMON, JOHN W. MINEAR*
and
DAVID H. JOHNSTON
Dept. of Earth and Planetary Sciences,
Massachusetts Institute of Technology,
Cambridge, Mass., U.S.A.

Abstract. The thermal history and current state of the lunar interior are investigated using constraints imposed by recent geological and physical data. Theoretical temperature models are computed taking into account different initial conditions, heat sources, differentiation and simulated convection. To account for the early formation of the lunar highlands, the time duration of magmatism and present-day temperatures estimated from lunar electrical conductivity profiles, it is necessary to restrict initial temperatures and abundances of radioactivie elements. Successful models require that the outer half of the Moon initially heated to melting temperatures, probably due to rapid accretion. Differentiation of radioactive heat sources toward the lunar surface occurred during the first 1.6 billion years. Temperatures in the outer 500 km are currently low, while the deep interior (radius less than 700 to 1000 km) is warmer than 1000°C, and is of primordial material. In some models there is a partially melted core. The calculated surface heat flux is between 25 and 30 erg/cm^2 s.

1. Introduction

The temperature of the interior of a planetary body is one of the most important parameters for determining the physical condition and chemical composition from geological and physical observations. In the absence of ways of reliably measuring internal temperatures directly, it is necessary to rely on theoretical calculations of the thermal evolution of the whole body. Further, such computations often provide tests for theories of planetary formation. The calculated thermal history of a planet depends strongly on the assumed initial conditions, input parameters and geological constraints. As these constraints change, new calculations must be carried out. In this paper we compute thermal-evolution models for the Moon taking into account new data from Apollo 11–15 Missions that are pertinent to this problem.

The thermal history of the Moon is not a new subject. Many investigators have computed temperature evolution models. (An incomplete list could include: Urey, 1952; MacDonald, 1959; Levin, 1962; Anderson and Phinney, 1967; Fricker *et al.*, 1967; McConnell *et al.*, 1967; Hanks and Anderson, 1969; Reynolds *et al.*, 1971; and Wood, 1971). Even since the most recent of these papers have been completed, new data of considerable importance to the thermal constraints have become available. Most notable among these are the lunar heat-flow measurements (Langseth *et al.*, 1971), electrical conductivity of the Moon and its thermal implication (Sonett *et al.*, 1971; and others), additional rock ages, and data on lunar seismicity and tectonism (Latham *et al.*, 1971). Those new data further constrain the lunar thermal models, and warrant a new set of calculations.

* Presently at the Research Triangle Institute, Research Triangle, North Carolina 27709, U.S.A.

Communication presented at the Conference on Lunar Geophysics, held between October 18–21, 1971, at the Lunar Science Institute in Houston, Texas, U.S.A.

The available data impose some definite boundary conditions and what might appear at times to be conflicting requirements on the past and present-day temperature models of the lunar interior. The existence of anorthosite rock sample from the Apollo 15 frontal site gives support to the idea that anorthosite is a major constituent of the lunar highlands (Wood *et al.*, 1970), which are relatively older than the mare basins. The age of the Apollo 15 anorthosite (rock No. 15415) is determined to be 4.1 b.y. (billion years), indeed older than any other lunar rock dated (Husain *et al.*, 1972). Plagioclase-rich highlands require extensive differentiation (*i.e.*, high temperatures and melting) at the very early history of the Moon. The ages of lunar basalts (3.2 to 3.9 b.y.) require that over an extended period of time the temperatures in the lunar interior have been near the melting curve of these rocks.

The data which point to present conditions, however, imply a relatively cold Moon. Electrical conductivity estimates seem to suggest temperatures less than 1000 °C everywhere in the lunar interior (Sonett *et al.*, 1971; Dyal and Parkin, 1971). The high viscosity, in excess of 10^{25} to 10^{27} poise (Baldwin, 1971), required to support the lunar mascons and other features is in accord with low temperatures at least within the outer few hundred kilometers of the Moon. The lunar seismic energy release is lower by about six orders of magnitude than in the Earth (Latham *et al.*, 1971) suggesting again the absence of thermally induced tectonic activity of any significance. These observations are contradicted by a high value of surface heat flow, about 33 ergs/cm^2 s (Langseth *et al.*, 1971). The above results will be the main constraints in our choice of acceptable thermal models.

In the computations we use a finite-difference scheme to solve the conservation-of-energy equation for a spherically symmetrical Moon. We allow for melting and differentiation, and allow for convection of molten material with the approximate scheme of Reynolds *et al.* (1966). Separately we consider the effect of convection by solid-state creep on our final temperature estimates.

In the paper, we first discuss the initial conditions, physical parameters, and heat sources which are most important inputs in any thermal calculation. The computational technique is described next in Section 3. Different temperature models are discussed in Section 4. These are followed by the conclusions in Section 5.

2. Initial Conditions and Input Parameters

The most important parameters for the thermal calculations are: (1) initial conditions, (2) heat sources – their temporal and spatial distribution, (3) thermal conductivity and its variations with temperature and pressure. In this section we discuss each item separately.

A. INITIAL CONDITIONS

The initial temperatures of the Moon are dependent on the lunar origin, mode of formation and the conditions associated with early history of the solar system. More specifically, these include gravitational heating due to accretion, short-lived radio-

activity, tidal dissipation, solar-wind flux, and compressional heating. None of these, except possibly tidal forces, would contribute appreciably to heating the Moon after its formation.

Most of these heat sources can be shown to have relatively small effects in the early history of the Moon. Heating by short-lived radioactivity is important only in the first 10^8 yr after nucleogenesis (Fish *et al.*, 1960). Lunar-origin theories, except the capture hypothesis, favor the Moon forming after the accretion of the Earth. Furthermore, the lack of Xe^{129} due to the decay of I^{129} on the Earth seems to necessitate at least 5×10^7 yr between nucleogenesis and the start of accretion (Anderson and Phinney, 1967).

Heating by tidal dissipation is a function of the lunar orbit soon after the Moon's formation. Estimates of its effect have varied from none at all (Singer, 1970) to enough to cause extensive melting (O'Keefe, 1970) and do depend on the theory of origin. Heating by an electric current produced by a uni-polar generator driven by the solar wind (Sonett *et al.*, 1968) would contribute to initial heating only if the Sun passed through a T-Tauri stage, characterized by mass loss and a high solar-wind flux. The adiabatic correction for compressional heating is easily calculated and would amount to only a few tens of degrees.

The most promising initial heating source, which could provide sufficient energy for melting near the surface regions of the Moon, is gravitational energy of accretion. Suppose that at some time t during accretion the proto-Moon has radius r, and that during a time increment dt an outer shell of thickness dr is added to the lunar mass. Then the temperature T within that shell may be estimated by equating the additional gravitational potential energy to radiated energy plus heat, namely,

$$\varrho \frac{GM(r)}{r} dr = \varepsilon\sigma (T^4 - T_b^4)\, dt + \varrho C_P (T - T_b)\, dr, \tag{1}$$

where ϱ is the density of the accreting particles, G is the gravitational constant, $M(r)$ is the mass of the body within radius r, σ is the Stefan-Boltzman constant, ε is the emissivity (here taken equal to 1), and C_P is the specific heat. T_b is the base temperature of the accreting particles, or the equilibrium temperature of the cloud of material within which the Moon formed; any effects of short-lived radioactivity are included. Numerous accretion rates, constant and varying, have been assumed in earlier papers (Ter Haar, 1948; Hanks and Anderson, 1969). A physically reasonable model, suggested by Hanks and Anderson (1969) and used in this paper (Figure 1a), is one in which the rate is slow in the beginning, increases as the accreted mass increases and then tapers off to zero as the material is depleted and the final planetary radius is achieved. The accretion rate is expressed by:

$$dr/dt = ct^2 \sin \gamma t. \tag{2}$$

The constants c and γ are determined from the Moon's radius R and the duration

of accretion τ:

$$\gamma = \frac{\pi}{\tau} \tag{3}$$

$$c = \frac{R\gamma^3}{\pi^2 - 4}.$$

Using this model, one can show that the near-surface temperatures never exceed the melting curve for accretion times greater than about 1000 yr. This conclusion is also reached by Mizutani *et al.* (1972) from a more detailed analysis of the accretion

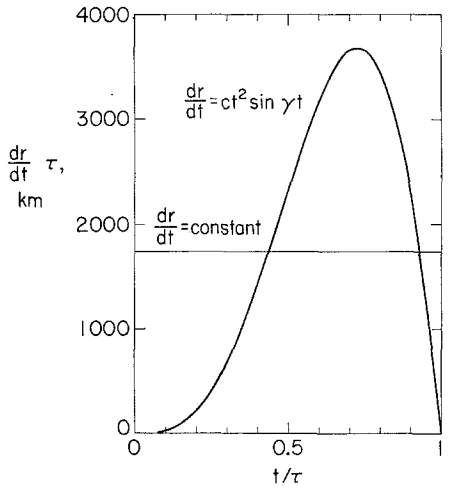

Fig. 1a.

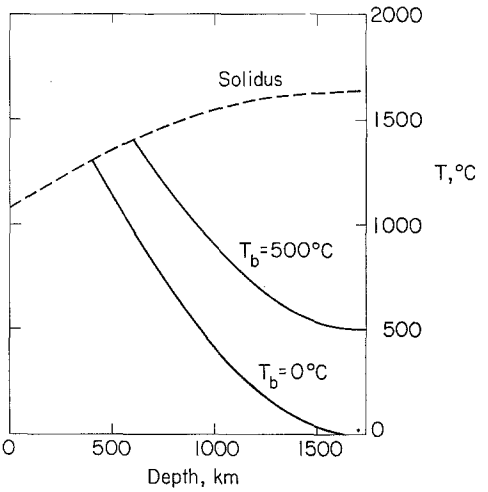

Fig. 1b.

Figs. 1a–b. (a) Two proposed models for the increase in lunar radius r with time t during accretion (from Hanks and Anderson, 1969). τ is the total accretion time. (b) Initial temperature profiles for a Moon accreting with a time-dependent radius growth and with base temperatures of 0° and 500 °C. Total accretion time is 100 yr. The solidus of dry basalt (Cohen *et al.*, 1967) is assumed to be an upper limit for possible initial temperatures.

process. One can estimate the duration of accretion by matching this model to the temperatures required to cause melting to a specified depth. To differentiate an anorthosite crust about 10 km thick requires melting to a depth of about 500 km. This can be achieved if the total accretion time is about 100 yr. Total accretion time may be made arbitrarily long, however, by appropriately lowering the assumed emissivity of the lunar surface. The temperature profile resulting from Equations (1) through (3) for a 100-yr accretion time is given in Figure 1b for two separate base temperatures; these profiles are adopted as starting temperatures in the calculations below.

B. HEAT SOURCES

The most important heat source in the thermal history calculations is the heat generated by the long half-life radioactive isotopes U^{238}, U^{235}, Th^{232}, and K^{40}. Although the abundances of these isotopes have been measured in the returned lunar samples (see Hays, 1971), determining the original concentration and distribution inside the Moon is difficult because of the complexities introduced by differentiation and magmatic enrichment. To determine initial abundances we must resort to indirect evidence.

In Figure 2, total K and U abundances are plotted for Apollo samples and some

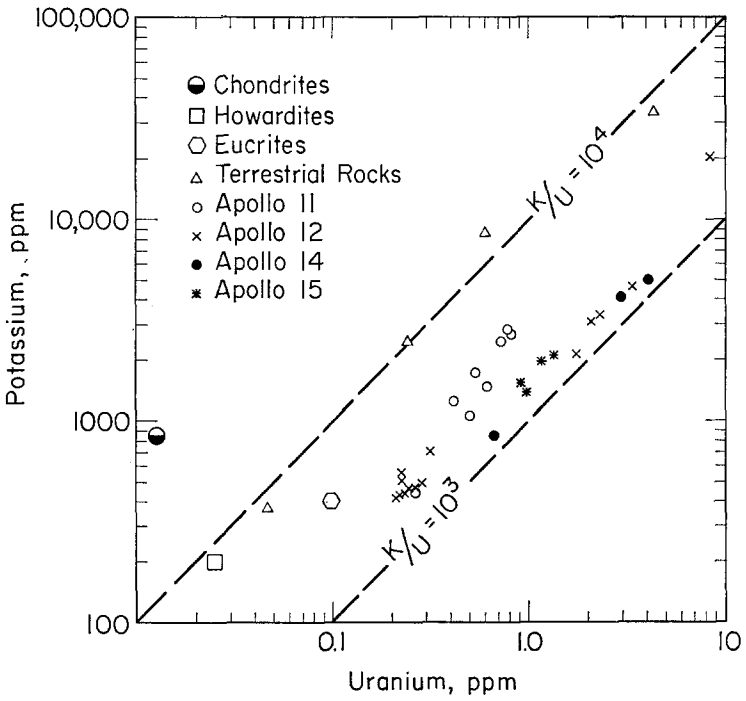

Fig. 2. Potassium and uranium concentrations in selected meteorites and lunar and terrestrial rocks, modified from Hays (1971). Points for eucrites, howardites, and Apollo 15 rock are from, respectively, Mason and Melson (1970), Duke and Silver (1967), and LSPET (1971).

terrestrial basalts and meteorites. It is clear that for all lunar rocks (including basalts breccias, and soils) the K/U ratio is about 2000, although absolute abundances vary. This compares with $K/U = 10000$ for the Earth and 80000 for the chondrites. The low K/U ratio presumably results from a depletion of volatile elements in the Moon (LSPET, 1969). It is clear that neither terrestrial nor chondritic abundances should be used for lunar calculations, as was done in some earlier studies. Chondrites could also be rejected on the basis of *Rb* abundances as a model for the primitive lunar material (Papanastassiou and Wasserburg, 1971). The Th/U ratio for lunar rocks is about 3.6 to 4.0, consistent with terrestrial and chondritic values.

To determine the absolute abundances we turn to achondrites and consider especially howardites and eucrites. The arguments for achondritic source material has been made directly and indirectly by a number of investigators (Duke and Silver, 1967; Hohenberg *et al.*, 1967). Howardites, which may be more typical than eucrites of average achondritic material, have a U abundance of 2.3×10^{-8} g/g (Duke and Silver, 1967) while for eucrites, which are enriched in refractory elements, the value is about 9.9×10^{-8} g/g. Our calculations show that a eucritic Moon would be almost completely molten at the present. Such a source material may be rejected on these grounds.

In this paper we assume howardite abundances (2.3×10^{-8} g/g) for U, and use $K/U = 2000$ and $Th/U = 4$. A few models have been calculated with higher and lower absolute U abundances and these are discussed in Section 4.

C. THERMAL CONDUCTIVITY

The effective thermal conductivity (including lattice conduction and radiative heat transfer) for some lunar terrestrial materials as well as theoretical estimates (MacDonald, 1963; Schatz, 1971) are shown in Figure 3. Clearly, lunar basalts cannot be used since they do not represent the bulk lunar composition (LSPET, 1969; Ringwood and Essene, 1970). In this study we adopt the curve given by Schatz (1971), which is based on laboratory measurements on single crystals and polycrystalline aggregates of olivine. At low temperatures, the conductivity is primarily due to lattice conduction and it decreases with increasing temperatures. At higher temperatures, the radiative term, roughly linear with temperature, is dominant. Previous studies of thermal evolution of the Moon have generally used MacDonald's formulation and assumed incorrectly that the opacity is constant with temperature; this gives the radiative contribution a cubic dependence on temperature. The pressure effects are probably small at lunar pressures and are neglected. In the calculations an analytic expression has been used for the curve marked '*S*' and conductivity is adjusted at each step for appropriate temperature.

D. OTHER PARAMETERS

The melting curve, surface temperature, specific heat, heat of fusion, and density must be specified for calculations. Most petrological studies indicate that the lunar basalts were not crystallized in the presence of water. Experimental work (Ringwood

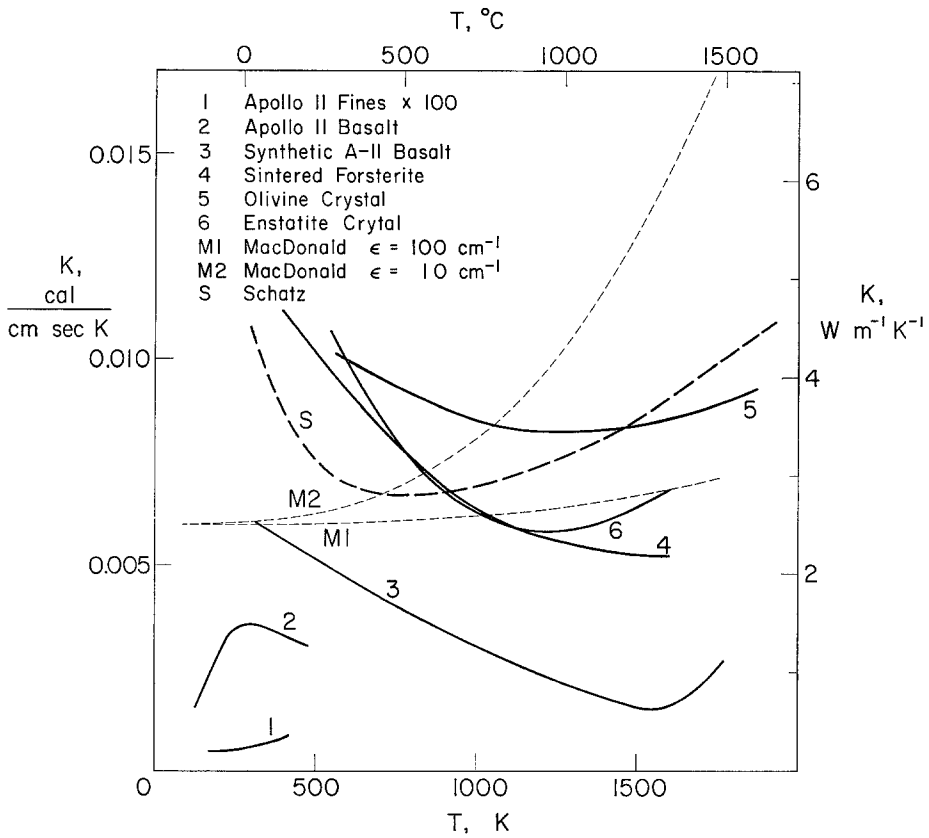

Fig. 3. Thermal conductivity of selected materials. Sources of measured data (solid lines) are Cremers (1971) for Apollo 11 fines, sample density 1.64 g/cm³; Horai *et al.* (1970) for Apollo 11 basalt; Murase and McBirney (1970) for synthetic Apollo 11 basalt; Schatz (1971) for sintered, polycrystalline forsterite and for single-crystal olivine (Fo_{86} Fa_{14}) and enstatite. Theoretical (dashed) curves include those of MacDonald (1963), for two different values of the mean extinction coefficient or opacity ε, and one proposed by Schatz (1971) for polycrystalline olivine of approximate composition Fo_{90} Fa_{10}. Schatz's (1971) curve, labeled *S* above, was adopted in this paper.

TABLE I

Parameters used in all thermal models

Radius	1740 km
Density	3.34 g/cm³
Heat of fusion	400 joules/g
Specific heat	1.2 joules/g°C
Surface temperature	−20°C
K/U ratio	2000
Th/U ratio	4

and Essene, 1970) suggest that melting of the Apollo 11 basalts is similar to terrestrial anhydrous basalts. The melting curve used in this paper is the solidus from the melting range of anhydrous basalts (Cohen *et al.*, 1967). We used only one curve to specify both partial and total melting; a constant density of 3.34 g/cm^3 and constant surface temperature of $-20\,^\circ$C (Langseth *et al.*, 1971) have been used. All other parameters are listed in Table I.

3. Computational Technique

The thermal calculations are carried out for a spherically-symmetric Moon (parameters varying with radius only at a given time), taking into account melting, simulated convection and differentiation. In this section these steps are described briefly.

Temperature models are calculated using the finite-difference solution of the heat conduction equation

$$C_P \varrho \frac{\partial T}{\partial t} = \frac{1}{r^2} \frac{\partial}{\partial r} \left(r^2 K \frac{\partial T}{\partial r} \right) + H(r, t), \tag{4}$$

where C_P is the specific heat, ϱ is the density, T is the temperature, r is the radius, K is the thermal conductivity, and $H(r, t)$ is the heat-source term. The coefficient K is taken to be temperature-dependent as discussed in the previous section, and heat sources may depend on radius and time.

The finite-difference analog of Equation (4) is given in the Appendix. Heat flux is conserved in the differencing technique. Since the scheme is explicit, a stability condition relating the time increment and the grid spacing must be fulfilled. The stability condition which is developed in the Appendix is

$$\Delta t < \frac{C_P \varrho \Delta r^2}{2K_{\max}} \frac{n^2}{(n + \frac{1}{2})^2}, \tag{5}$$

where $K_{\max}$ is the maximum value of the conductivity at a given time step. The time increment is computed at each time step using Equation (5) with a factor of 4 instead of 2 in the denominator. Generally a grid spacing of 20 km is used. This is reduced to 5 km at later stages of calculations for more accurate determination of near surface temperature and heat flux.

To avoid problems with the temperature becoming infinite at the center of the Moon ($r=0$), the solution was started at $r=20$ km. Heat flux was taken as zero at the grid point corresponding to $r=20$ km by setting $T_1^n = T_2^n$ where T_1^n is the temperature at $r_1 = 20$ km and T_2^n is the temperature at $r_2 = r_1 + \Delta r$. Temperature was kept constant ($-20\,^\circ$C) at the surface of the Moon. Surface heat flux was computed using a parabolic fit to the temperature at three grid points starting with the surface point.

The computational scheme was tested against exact solutions for a radially symmetric sphere with constant heat production and heat production varying sinusoidally with radius. Agreement between the finite-difference and the exact solution was excellent with temperatures differing by less than 0.2% after 2.5 billion years in the case of constant heat production.

A. SIMULATION OF MELTING AND CONVECTION

The effects of melting and convection on temperature were modeled using a technique described by Reynolds *et al.* (1966). In this technique, the temperature profile at some time $m\Delta t$ is compared with a given melting-point curve. If the tempereture T_n^m is above the melting point, T_n, the temperature increment above the melting point $(T_n^m - T_n)$ is converted to its heat equivalent, ΔH, by dividing by the specific heat and the density. If ΔH is not equal to or greater than a specified heat of fusion, the material is taken as partially molten, the temperature at point $n\Delta r$ is held at T_n and another iteration in time performed. The material at point $n\Delta r$ remains partially molten at temperature T_n until the sum of the ΔH's from $m\Delta t$ to some $(m+p)\,\Delta t$ equals the heat of fusion. At this point in time the material is completely molten and temperature is allowed to increase above T_n. Provision is made for the phase change to run either way so that molten material may solidify by releasing heat equal to this heat of fusion.

Convection simulation uses the same technique as does melting except that once the material has become completely molten, temperature is held at the melting point. Any increase in temperature which would raise the temperature above the melting point is converted into its heat equivalent and transferred upward to the next grid point as an equivalent temperature increment due to convection. The conversion to equivalent heat and back to temperature is necessary since the volume element increases with radius.

The main assumption underlying this technique is that convection occurs on complete melting and limits the temperature in the region of complete melting to the melting temperature. This scheme accounts for the transfer of heat which would have taken place under convection without actually using the mass transfer terms in the equation.

B. DIFFERENTIATION

In the regions where melting occurs, the magma would be enriched with *U*, *Th* and *K* and eventually would transfer these heat sources toward the surface. To account for this, at discrete time steps the heat sources from the molten zones were differentiated upwards. Where no melting occurred no differentiation was carried out and initial radioactive abundances were maintained.

The concentration of radioactive heat sources after differentiation was assumed to decrease exponentially with depth (Lachenbruch, 1968) as

$$H(r) = A_0 e^{-(R-r)/h},$$

where A_0 is the surface abundance, R is the lunar radius, and h is a skin depth. For a skin depth of 10 to 20 km, reasonable agreement was found between the calculated surface abundance A_0 and the average (taking into account mare and highlands) of observed surface-rock concentrations. Differentiation was carried out in 2 to 3 steps, starting with $h=200$ km and decreasing to $h=10$ km at $t=1.6$ b.y. The last differentiation was assumed to take place 3.0 b.y. ago.

4. Temperature Models

We now consider specific models for the thermal evolution of the Moon. Unless stated otherwise, in all models below the thermal conductivity is taken to equal to curve *S* (Schatz, 1971) in Figure 3; the bulk concentration of uranium in the Moon is

TABLE II

A summary of model parameters for all models

Fig. No.	Base temp. °C	Accretion heating included?	*U* concentration (10^{-8} g/g)	Conductivity model	Melting at present	Surface heat flux (ergs/cm²s)
4	0	No	1.1–3.3	*S*	No	–
5	0	Yes	2.3	*S*	Yes	24
7	500	Yes	2.3	*S*	Yes	25
8	800	Yes	2.3	*S*	Yes	27
9	Initially molten		2.3	*S*	No	29
10	500	Yes	2.3	*M*2	Yes	25
11	0	Yes	1.1	*S*	No	21
12 (convecting)	0	Yes	2.3	*S*	No	25

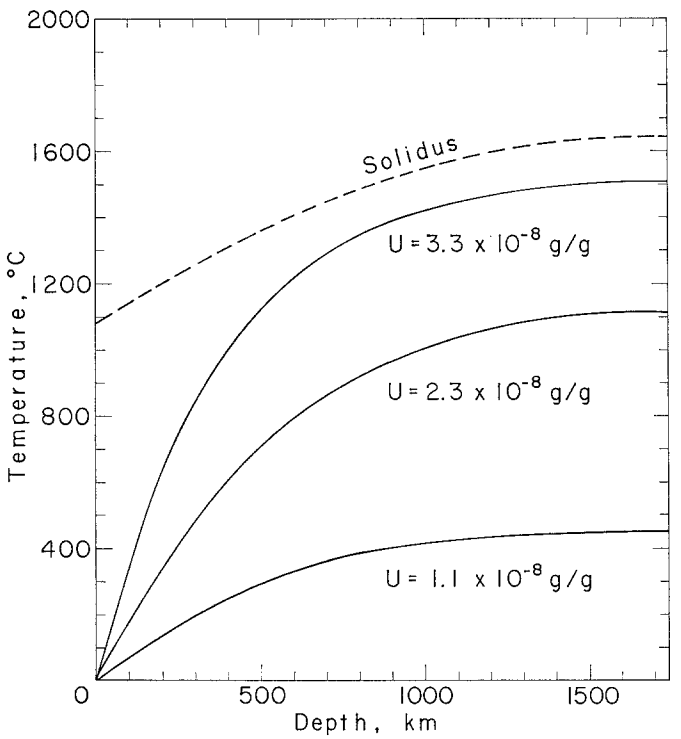

Fig. 4. Final temperature profiles in an initially-cold Moon (0°C at all depths) as a function of present-day concentration of uranium. The solidus of anhydrous basalt (Cohen *et al.*, 1967) is also shown.

set equal to 2.3×10^{-8} g/g; and heat transfer by convection and upwards concentration of radioactive heat sources are simulated when melting occurs. A summary of all the models with corresponding figures is listed in Table II.

A rough idea of the effect of such a uranium concentration may be gathered from Figure 4. In the figure, the present-day temperature in a uniform, initially cold ($T=0$ °C everywhere) Moon is shown as a function of the present-day concentration of uranium. For $U \leq 3.7 \times 10^{-8}$ g/g, the temperature is below the solidus of anhydrous basalt (Cohen *et al.*, 1967) throughout the Moon. Clearly models such as those in Figure 4 that begin with an everywhere-cold Moon cannot generate enough heat from radioactivity alone to provide the necessary melting and differentiation in the Moon's upper few hundred kilometers.

A more realistic temperature model is given in Figure 5. In the model, cold (0 °C) particles accrete to form the Moon in a time interval of 100 yr. This gives an initial temperature profile with melting and probable differentiation to depth of 420 km and a cold interior (radius < 1000 km). The evoluation of the temperature profile with time

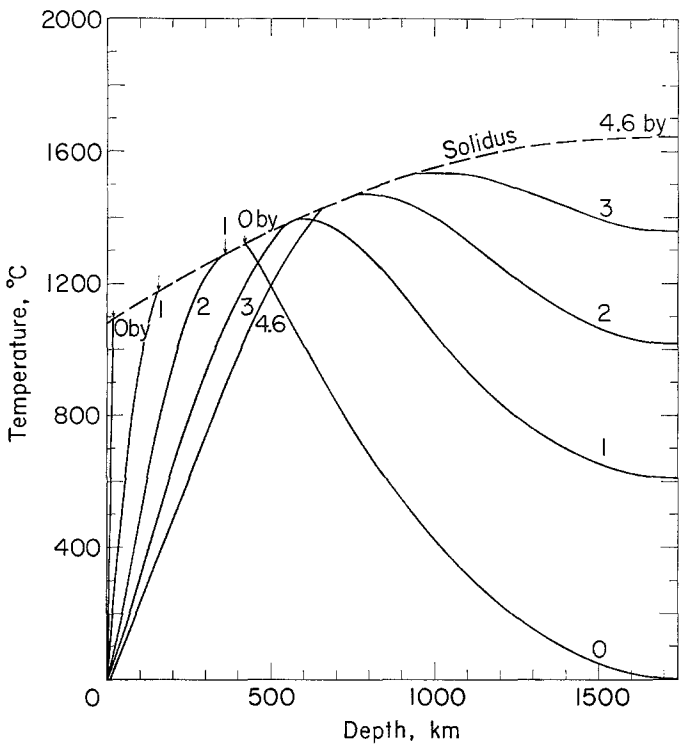

Fig. 5. A model of the evolution of the temperature profile in the Moon as a function of time since lunar origin. The initial temperature profile is from Figure 1, with a base temperature of 0 °C. The Moon is partially or completely molten at those depths where the temperature profile lies along the solidus of anhydrous basalt (Cohen *et al.*, 1967). The depth range for complete melting is delimited by the small arrows above the solidus. Time, in billions of years, is indicated by the number adjacent to each profile.

is shown in Figure 5. In this model, the outer portions of the Moon cool monotonically with time while the interior progressively warms. Partial melting occurs at some depth over the entire lunar history. At present in the model the Moon is partially molten below 650 km and the average heat flow through the Moon's surface is 24 erg/cm^2 s.

The extent of melting in the outer 700 km of the Moon is better viewed in Figure 6, where we have shown the depth interval over which partial and complete melting occur in the thermal model as a function of time since lunar origin. The solid rind or lithosphere of the Moon increases in thickness with time at the approximate rate of 170 km/b.y. Thus, if the time of mare formation is limited by the ages of Apollo basalts (3.2 to 3.9 b.y.), then the lithosphere was 115 to 235 km thick at that time. This agrees with estimates for the depth of origin of lunar basalts (Ringwood and Essene, 1970) and accounts for the rigidity of the outer layers of the Moon required to support the mascons (Urey, 1968). Presumably only the impact of a large body could excavate and weaken the lithosphere to the extent necessary to allow the molten component of the hotter material beneath to escape to the surface.

The effects of somewhat different initial conditions are shown in the next three models. Parameters of the model in Figure 7 are identical to those of Figure 5 except that the temperature of the particles that accreted to form the Moon is taken to be 500 °C. This raises the initial temperature profile at all depths below 400 km; initial melting extends to a depth of 630 km. The temperature profile as a function of time is

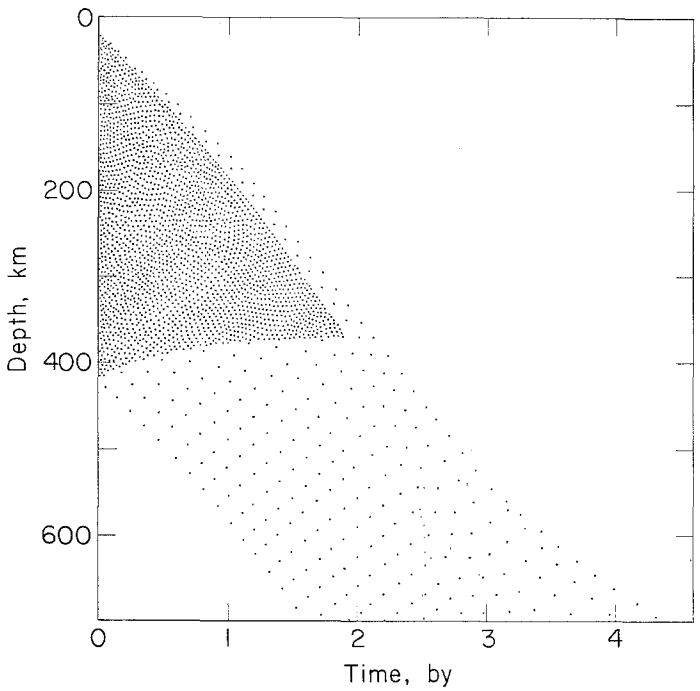

Fig. 6. The extent of melting in the thermal model of Figure 5. Heavy stippling denotes complete fusion; lighter stippling denotes only partial fusion.

very similar to the previous model at depths less than 250 km. Below about 500 km, the Moon heats more quickly to the solidus than in the previous model and, because of the more efficient transfer of heat upon melting, is generally cooler at the present. The Moon is currently solid to a depth of 1100 km in this model, and the surface heat flow at present is 25 erg/cm^2 s.

In Figure 8 is shown a temperature model which begins with melting extending to a depth of 900 km. The initial temperature profile below 900 km depth, though not strictly obtained from an accretion model, is of the same general shape as in models considered earlier. Again, the outer 250 km behaves similarly in this model and in those of Figures 5 and 7. The center of the Moon heats to the solidus in about 2 b.y. The outer 1000 km of the Moon are solid at present, and the surface heat flow is 27 erg/cm^2 s.

As an extreme case, we consider an initially molten Moon in Figure 9. In this model, all the radioactive elements are concentrated near the lunar surface at time zero. Because of the depletion of heat sources in the interior and because of the efficient heat transfer in the molten regions, the Moon in this model cools more rapidly than in previous models. The lithosphere grows in thickness at a rate of 200 to 250 km/b.y. and the Moon is entirely solid and cooling everywhere at the present time. The final surface heat flow is 29 erg/cm^2 s.

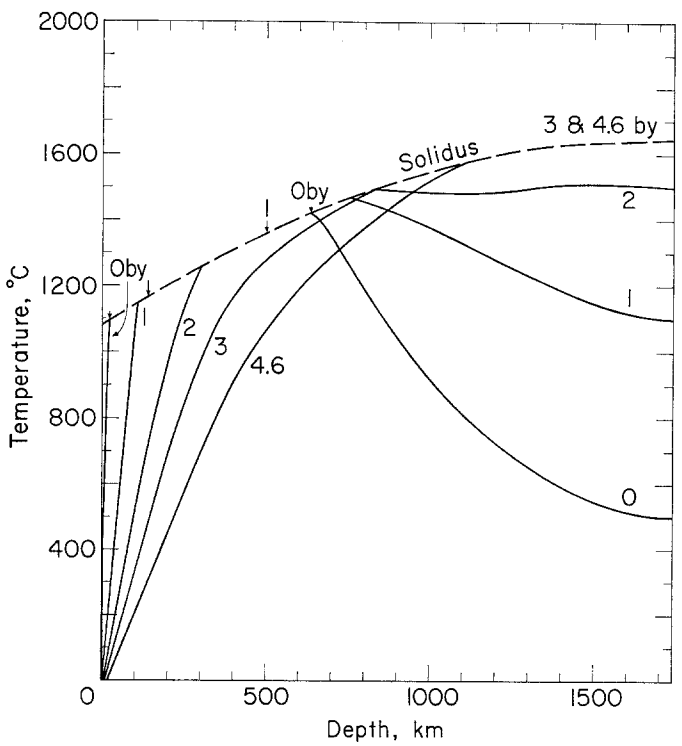

Fig. 7. Thermal evolution in a Moon accreted at a base temperature of 500°C. All other parameters and symbols are identical to those of Figure 5.

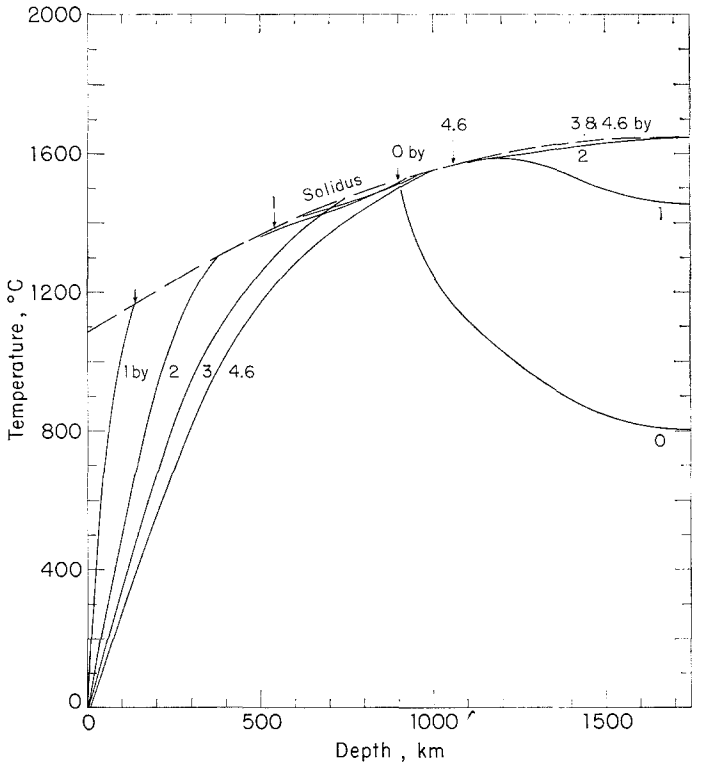

Fig. 8. Thermal evolution in a Moon initially melted to a depth of 900 km. All other parameters and symbols are identical to those of Figure 5.

Details of the thermal evolution are sensitive to the adopted values of thermal conductivity as a function of temperature. In Figure 10 is shown a model with physical parameters equal to those of Figure 7 except that the thermal conductivity is taken to equal approximately curve M_2 (MacDonald, 1963) of Figure 3. This appreciably increases the efficiency of heat transfer at temperatures greater than 500 °C. Thus the outer portions of the Moon cool more rapidly than in the model of Figure 7 and there exists a period from about 2 to 2.5 b.y. after lunar origin when the Moon was entirely solid. At present, in the model, there is a small partially molten core of radius 300 km and the surface heat flow is 25 erg/cm^2 s.

The final temperature profiles in all of the above models with some initial melting are reasonably similar. At depths greater than 1000 km, temperatures are within 100 °C of the basalt solidus in all of these models. A partially molten core is present in all models except those with extreme initial conditions or physical properties. The greatest difference among present-day temperatures in the models occurs between 300 and 700 km depth and amounts to no more than 350 °C.

These present-day temperatures are fairly high: temperatures exceed 1000 °C at depths ranging from 400 to 600 km. Thus these thermal models are at odds with many of the recent estimates of lunar temperature from measurements of electrical conduc-

tivity in the Moon (Sonett *et al.*, 1971; Dyal and Parkin, 1971; Sill, 1971), unless a resistive material such as enstatite is assumed for the major constituent of the lunar mantle (Sill, 1971).

One means of generating temperature models which are cooler at present is to postulate a lower bulk concentration of radioactive heat sources for the Moon. In Figure 11 is shown the temperature profile as a function of time in a model that is identical in physical parameters with the model of Figure 5 except that the bulk concentration of uranium in the Moon today is assumed to be 1.1×10^{-8} g/g. In the model of Figure 11, the upper 400 km cool somewhat more quickly and the lowest 1200 km heat considerably slower than in the more radioactive model. The Moon solidifies completely within 2 b.y. after formation in this model. Because below 400 km the Moon is undifferentiated, the interior of the Moon (radius <800 km) is still heating at present. The final surface heat flow is 21 erg/cm^2 s.

In all of the models above, heat transfer by convective mass transport was ignored at sub-solidus temperatures. This is probably unreasonable. Several authors (Runcorn, 1962; Kopal, 1962; Turcotte and Oxburgh, 1969b; Tozer, 1971) have argued persuasively that convection by solid-state creep should be at least as efficient a heat-transfer mechanism as lattice conduction and radiation at temperatures considerably below

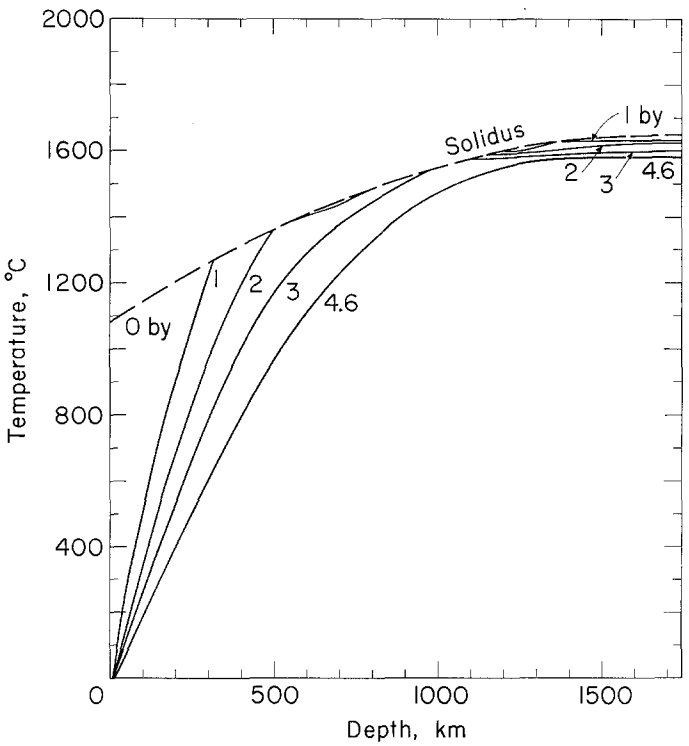

Fig. 9. Thermal evolution in a Moon initially molten. All other parameters and symbols are identical to those in Figure 5.

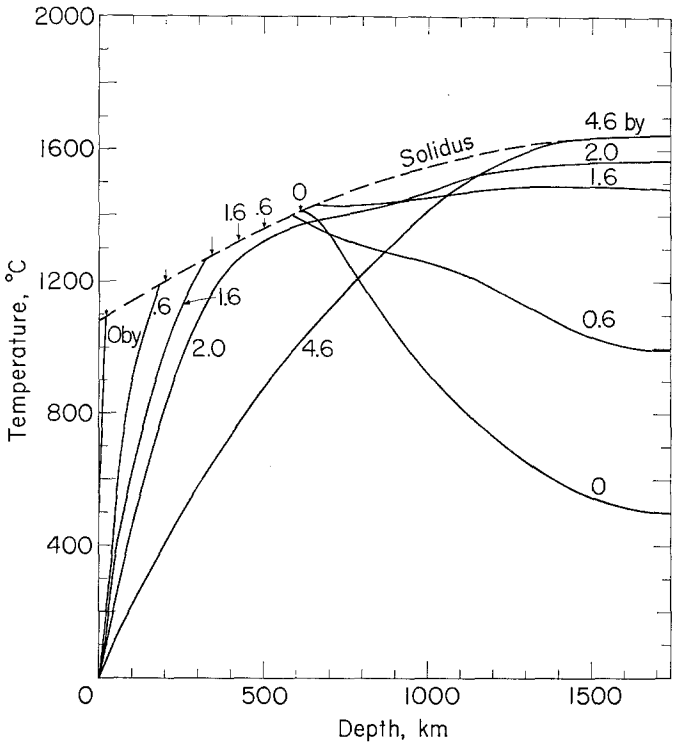

Fig. 10. Thermal evolution in a Moon with an artificially high thermal conductivity (approximately curve *M*2 of Figure 3). Parameters otherwise equal to those of Figure 7. For explanation of symbols, see Figure 5.

the solidus. Inclusion of the effect of solid-state creep should produce present-day temperature profiles that are cooler than those given above.

While we cannot solve the complete problem of thermal evolution in a realistically convecting Moon, we can make some simplifying assumptions that allow us to make a zero-order estimate of the effect of solid-state creep on our thermal history calculations. Convective solutions to the present temperature profile in the Moon generally show a stable shell of a few hundred kilometers overlying a convecting interior of nearly constant viscosity (Turcotte and Oxburgh, 1969b; Tozer, 1971), a consequence of the low pressures and small adiabatic temperature gradient in the Moon. We therefore postulate in our thermal evolution models that solid-state creep will be an efficient heat transfer mechanism when the temperature in the bulk of the lunar interior is such that the viscosity exceeds a critical value. This temperature is essentially the 'stabilization temperature' of Tozer (1970, 1971). Convection is simulated, as before, as a 100%-efficient process: all heat in excess of that required to maintain the viscosity of the material at the critical value is transferred upward in the model. We assume a rheology proposed by Turcotte and Oxburgh (1969a) for diffusion creep in the Earth's mantle. Thus we ignore the probable complication of non-Newtonian

viscosity (Weertman, 1970), an uncertain increase in viscosity associated with the depletion of volatiles in the Moon relative to the Earth (Orowan, 1965), and the apparent conflict between geophysical constraints on the rheology of the Earth's mantle and presently available laboratory measurements of high-temperature creep in rocks (Goetze and Brace, 1971). Two values for the critical value of viscosity were chosen: 10^{21} and 10^{24} poise. The first was predicted for the lunar interior by Turcotte and Oxburgh (1969b) on the basis of their boundary-layer theory and is also within an order of magnitude of values often cited for the viscosity of the Earth's upper mantle. The second value is an estimate, obtained from marginal stability theory in a uniform, gravitating sphere, of the maximum value permissible if the Moon is currently convecting (Turcotte and Oxburgh, 1969b). We found that using a value of 10^{21} poise for the critical viscosity did not alter significantly the thermal evolution from models similar in all respects but neglecting solid-state creep; this is because the temperatures at which such a viscosity is reached, according to the viscosity-temperature relationship of Turcotte and Oxburgh (1969a), are very near the basalt solidus of Cohen *et al.* (1967). Thus only a model which convects when the viscosity is less than 10^{24} poise throughout most of the Moon is considered below.

Such a model is shown in Figure 12. This model is identical to that in Figure 5 for

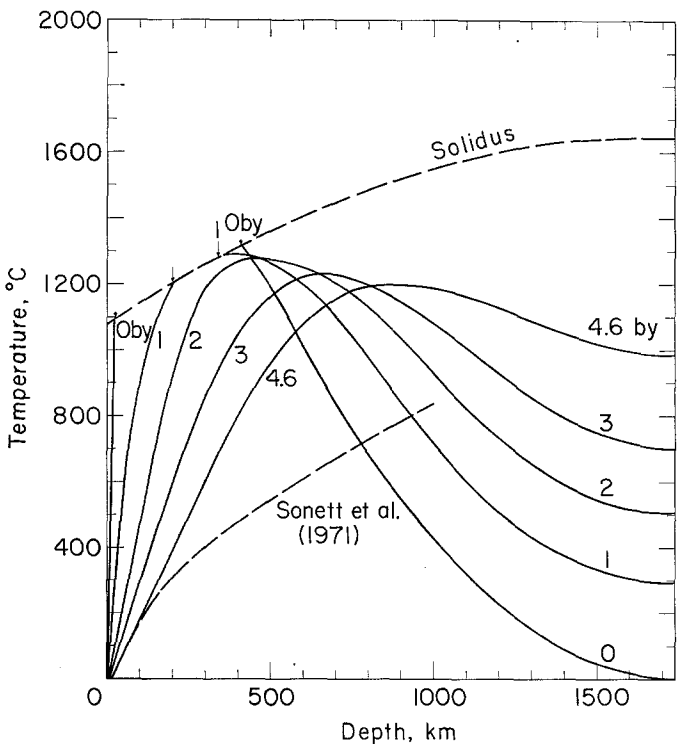

Fig. 11. Thermal evolution in a Moon with a present-day uranium concentration of 1.1×10^{-8} g/g. All other parameters and symbols are as in the model of Figure 5.

the first 2 b.y. At that time, almost all of the Moon below 250 km depth is at a temperature high enough to give a viscosity less than 10^{24} poise. Although the viscosity was less than that value over a more limited depth range at times less than 2 b.y., we argue that solid-state creep was probably unimportant at these early stages

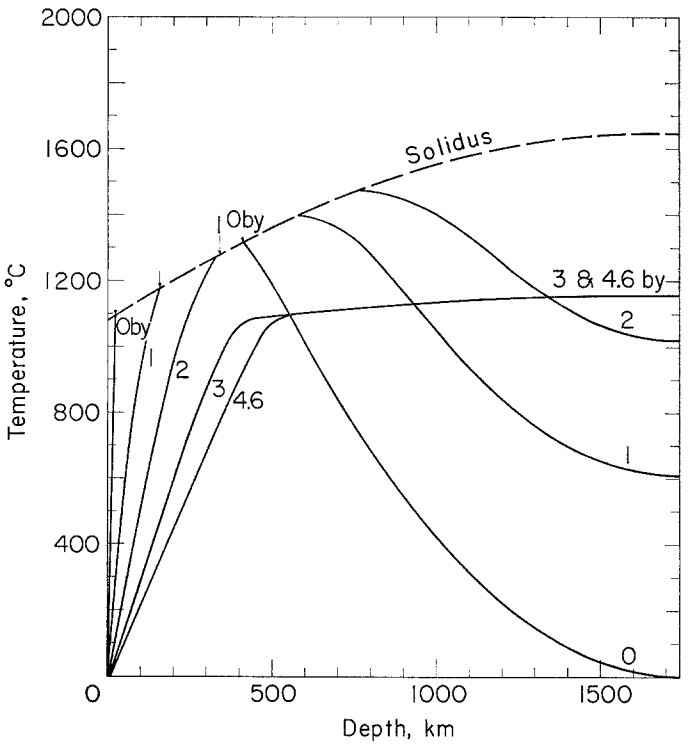

Fig. 12. The effect of convection by solid-state creep on the later stages of thermal evolution in the Moon (see text). From 0 to 2 b.y., this model is identical to that of Figure 5.

by appealing qualitatively to the very strong dependence of the Rayleigh number, a criterion for hydrodynamic instability, on the characteristic length (depth interval) of the convective cell (e.g., Turcotte and Oxburgh, 1969b). After 2 b.y. in the model (Figure 12), the temperature in the convecting interior is stabilized at that temperature necessary to maintain a viscosity of 10^{24} poise; the gradient is slightly superadiabatic. All excess heat is transferred to the non-convecting outer shell, which is slowly cooling and thickening with time. The present-day heat flow at the lunar surface in this model is 25 erg/cm^2 s.

5. Discussion and Conclusions

In this paper we studied the thermal evolution of the Moon from three basic initial models: (a) A Moon initially cold, (b) A Moon accreted hot and initially molten

everywhere, and (c) A Moon accreted relatively rapidly so that the outer few hundred kilometers were at near-solidus temperatures while the interior was relatively cold. The results of our computations indicate that:

(1) An initially cold Moon (Figure 4) would neither melt nor differentiate to account for the lunar crustal rocks and basalts with any plausible radioactive heat-source abundances. Thus it is not an acceptable model.

(2) An initially molten Moon would have cooled below the solidus at the present time. While such a model is consistent with the majority of thermal constraints, there are a number of other complications (e.g., Ringwood, 1970), and this model is not favored.

(3) Moon models based on rapid accretion satisfy the requirements for early and extended periods of magma generation. Thermal evolution for such models follows a characteristic pattern, where, with increasing time, the outer part of the Moon cools while the inner portion heats up. Melting progresses downward. At 4.6 b.y. most models have a partially molten core of the same composition as the initial primordial lunar material.

(4) Addition of sub-solidus convection at high temperatures eliminates melting at the center, without altering the general shape of the above temperature curves. The surface effects of such a model will be the same. Near the surface where temperatures are relatively low, convection is not an important factor in heat transfer.

(5) Our computations indicate that a Moon model that is initially molten and differentiated to a depth of 600–800 km satisfies the geologic, geophysical and geochronologic constraints for the formation of a lunar crust and mare basalts. During the first 2 b.y. of lunar history, the top of the partially molten zone remains within 300 km of the lunar surface. At the present time, these models give an average surface heat flow of about 25 to 30 erg/cm^2 s (see Table II) which is slightly lower than the measured value at the Apollo 15 site (Langseth *et al.*, 1971). It should be clarified that theoretical values do not take into account the contribution to heat flow by the radioactively enriched lunar soil which affects the measurement.

(6) The temperatures for the above models (in fact, for all the models we computed) are higher than the values of Sonett *et al.* (1971), as can be seen in Figure 11, unless we reduce the average U abundance to below 1.0×10^{-8} g/g (cf. Hays, 1971) and/or increase the conductivity to a value even higher than curve M_2 (Figure 3). Neither of these alternatives is acceptable. Considering the difficulties and uncertainties involved in estimating electrical conductivity and converting these to temperatures, it may be advisable to await further analysis and data before we are rigidly bound by this temperature model.

(7) Most of our models point to a transition zone between 600–1000 km depth (going from differentiated to undifferentiated, non-convecting to convecting, sub-solidus temperatures to partial melting). It is interesting that the largest and most persistent moonquakes (A-1 type events described by Latham *et al.*, 1971) have focal depths of about 800 km. The transition region beneath a cool and rigid lithosphere may indeed be the zone of deviatoric stresses.

Appendix

A. FINITE-DIFFERENCE EQUATION

The finite-difference analog of Equation (4) which conserves heat flux is

$$T_n^{m+1} = T_n^m + \frac{\alpha}{n^2 p^2}\left[(n+\tfrac{1}{2})^2 \frac{(K_{n+1}^m + K_n^m)}{2}(T_{n+1}^m - T_n^m) - (n-\tfrac{1}{2})^2 \frac{(K_n^m + K_{n-1}^m)}{2}(T_n^m - T_{n-1}^m)\right] + \alpha H_n^m, \tag{A1}$$

where $p = \Delta r$, $r = np$, $t = m\Delta t$, $\alpha = t/C_P\varrho$, $T_n^m = T(np, m\Delta t)$.

B. STABILITY

Equation (A1) may be expressed in matrix form as

$$\mathbf{u}^{m+1} = (\mathbf{I} + \mathbf{A})\,\mathbf{u}^m + \mathbf{H}^m, \tag{A2}$$

where $\mathbf{u}^{m+1}$, $\mathbf{u}^m$, and $\mathbf{H}^m$ are column vectors defined by

$$\mathbf{u}^{m+1} = (T_1^{m+1}, T_2^{m+1}, \ldots T_M^{m+1}),$$

and

$$\mathbf{H}^m = \alpha(H_1^m, H_2^m, \ldots H_M^m);$$

$\mathbf{I}$ is the identity matrix and $\mathbf{A}$ is the $(M \times M)$ matrix defining the finite-difference scheme given by

$$\mathbf{A} = \begin{pmatrix} -(B+C) & B & & & \\ C & -(B+C) & B & 0 & \\ & & \ddots & & \\ & 0 & C & -(B+C) & B \\ & & & C & -(B+C) \end{pmatrix}, \tag{A3}$$

with

$$B = \frac{\alpha(n+\tfrac{1}{2})^2 (K_{n+1} + K_n)}{2n^2 p^2}$$

and

$$C = \frac{\alpha(n-\tfrac{1}{2})^2 (K_n + K_{n-1})}{2n^2 p^2}.$$

If we express $\mathbf{u}^0$ in terms of the eigenvectors of $\mathbf{A}$

$$\mathbf{u}^0 = \sum_{k=1}^{M} \gamma_k \mathbf{w}_k \tag{A4}$$

and substitute in Equation (A2), we obtain

$$\mathbf{u}^m = (\mathbf{I} + \mathbf{A})^m \mathbf{u}^0 + \sum_{p=0}^{m-1} (\mathbf{I} + \mathbf{A})^{m-1-p} \mathbf{H}^p .$$

Expanding $\mathbf{H}^0$ in terms of the eigenvectors of $\mathbf{A}$

$$\mathbf{H}^0 = \sum_{k=1}^{M} \beta_k \mathbf{w}_k$$

and noting that $\mathbf{Aw} = \lambda \mathbf{w}$ we find that

$$\mathbf{u}^m = \sum_{k=1}^{M} (1 + \lambda_k)^m \gamma_k \mathbf{w}_k + \sum_{p=0}^{m-1} \sum_{k=1}^{M} (1 + \lambda_k)^{m-1-p} \beta_k \mathbf{w}_k . \tag{A5}$$

Therefore, $|1+\lambda_k| < 1$ if the difference scheme is to be stable. Noting that $\lambda_r = \mathbf{Aw}_r \cdot \mathbf{w}_r$ and using the expression for $\mathbf{A}$ given by Equation (A3), it can be shown that

$$\lambda_r = -\tfrac{1}{2} \sum_{p=0}^{M} (B + C) (w_{p+1,r} - w_{p,r})^2 \tag{A6}$$

by letting $w_{0,r} = w_{m+1,r} = 0$. Since B and C are positive, all of the eigenvalues of $\mathbf{A}$ are negative. Then letting

$$\begin{aligned} &\mathbf{u} = \sum_{k=1}^{M} \alpha_k \mathbf{w}_k , \\ &|\mathbf{Au} \cdot \mathbf{u}| = \alpha_1^2 |\lambda_1| + \alpha_2^2 |\lambda_2| + \cdots + \alpha_M^2 |\lambda_M| . \end{aligned} \tag{A7}$$

If the eigenvalues of $\mathbf{A}$ are ordered so that

$$|\lambda_1| < |\lambda_2| < \cdots |\lambda_M| ,$$

then

$$|\lambda_1| < \frac{|\mathbf{Au} \cdot \mathbf{u}|}{(\mathbf{u} \cdot \mathbf{u})} < |\lambda_M| . \tag{A8}$$

Thus, $|\mathbf{Au} \cdot \mathbf{u}|/(\mathbf{u} \cdot \mathbf{u})$ is bounded by the numerically least and greatest eigenvalues of $\mathbf{A}$. Analogous to Equation (A6), one has for any arbitrary vector

$$\frac{|\mathbf{Au} \cdot \mathbf{u}|}{(\mathbf{u} \cdot \mathbf{u})} = \tfrac{1}{2} \sum_{p=0}^{M} (B + C) (u_{p+1} - u_p)^2 \tag{A9}$$

if $u_0 = u_{M+1} = 0$. Letting K^* and K_* be the maximum and minimum values of B and C respectively, and $\mathbf{A}^*$ and $\mathbf{A}_*$ the corresponding $\mathbf{A}$, one has

$$\frac{|\mathbf{A}_* \mathbf{u} \cdot \mathbf{u}|}{(\mathbf{u} \cdot \mathbf{u})} < \frac{|\mathbf{Au} \cdot \mathbf{u}|}{(\mathbf{u} \cdot \mathbf{u})} < \frac{|\mathbf{A}^* \mathbf{u} \cdot \mathbf{u}|}{(\mathbf{u} \cdot \mathbf{u})} . \tag{A10}$$

The eigenvalues of $\mathbf{A}^*$ and $\mathbf{A}_*$ are

$$-4K^* \cos^2 \frac{k\pi}{2(M+1)}$$

and

$$-4K_* \cos^2 \frac{k\pi}{2(M+1)}, \quad k = 1, 2, 3, \cdots, M,$$

respectively (Lowan, 1957). Thus

$$1 - 4K^* \cos^2 \frac{k\pi}{2(M+1)} < 1 + \lambda_k < 1 - 4K_* \cos^2 \frac{k\pi}{2(M+1)}. \tag{A11}$$

If $|1+\lambda_k|<1$ then $K^*<\frac{1}{2}$, giving the stability criterion

$$\begin{aligned} &\frac{\Delta t}{C_{P\varrho}} \frac{(n+\frac{1}{2})^2}{n^2 \Delta r^2} K_{\max} < \tfrac{1}{2} \\ &\Delta t < \frac{C_{P\varrho}}{2K_{\max}} \Delta r^2 \frac{n^2}{(n+\frac{1}{2})^2}, \end{aligned} \tag{A12}$$

where $K_{\max}$ is the maximum value of the conductivity at the given time step.

C. CONVERGENCE

Let $U(r, t)$ be the exact solution of Equation (1). Expanding $U(r, t)$ in a Taylor series about $(n\Delta r, m\Delta t)$ and substituting the expansion into Equation (A1)

$$\frac{\partial U}{\partial t} = \beta \frac{2K}{r} \frac{\partial U}{\partial r} + \beta \frac{\partial K}{\partial r} \frac{\partial U}{\partial r} + \beta K \frac{\partial^2 U}{\partial r^2} + \beta H(r, t) - \Phi, \tag{A13}$$

where

$$\beta = 1 / C_{P\varrho}$$

and

$$\Phi = U_{,tt} \frac{\Delta t}{2} - \frac{\beta \Delta r^2}{4r} (K_{,r} U_{,r} + K U_{,rr}) + O(\Delta t^2, \Delta r^3). \tag{A14}$$

Letting $d_n^m = U(n\Delta r, m\Delta t) - T_n^m$, substituting into Equation (A1) and using Equation (A13) gives

$$\mathbf{d}^{m+1} = (\mathbf{I} + \mathbf{A})\, \mathbf{d}^m + \mathbf{\Phi}_m. \tag{A15}$$

The difference between the exact and finite-difference solutions satisfies the same equation as the finite-difference solution with $\mathbf{H}^m$ replaced by $\mathbf{\Phi}_m$.

For the finite-difference solution to be accurate as well as stable, $d_n^{m+1} \to 0$ as Δr and $\Delta t \to 0$. To begin, it is reasonable to assume that $d_n^0 = U(n\Delta r, 0) - T_n^0 = 0$. Therefore,

$$\mathbf{d}^{m+1} = \sum_{p=0}^{m} (\mathbf{I} + \mathbf{A})^{m-p} \mathbf{\Phi}_p. \tag{A16}$$

Expressing $\mathbf{\Phi}_p$ in terms of the eigenvectors of $\mathbf{A}$ so that

$$\mathbf{\Phi}_p = \sum_{k=1}^{M} C_k^{(p)} \mathbf{w}_k \tag{A17}$$

yields

$$(\mathbf{I}+\mathbf{A})^{m-p}\mathbf{\Phi}_p = \sum_{k=1}^{M} C_k^{(p)}\,(1+\lambda_k)^{m-p}\mathbf{w}_k\,,$$

which on substituting into Equation (A16) yields

$$\mathbf{d}^{m+1} = \sum_{k=1}^{M} \left[C_k^{(0)}(1+\lambda_k)^m + C_k^{(1)}(1+\lambda_k)^{m-1} + \cdots + C_k^{(m)}\right] \mathbf{w}_k\,. \tag{A18}$$

Letting d_h^{m+1} and $w_{h,\,k}$ be the h component of $\mathbf{d}^{m+1}$ and $\mathbf{w}_k$, respectively, produces

$$d_h^{m+1} = \sum_{k=1}^{M} \left[C_k^{(0)}(1+\lambda_k)^m + C_k^{(1)}(1+\lambda_k)^{m-1} + \cdots + C_k^{(m)}\right] w_{h,\,k}\,. \tag{A19}$$

From Equation (A17)

$$C_k^{(p)} = \mathbf{\Phi}_p \cdot \mathbf{w}_k = \frac{1}{M}\left(\Phi_{1,\,p} w_{1,\,k} + \cdots + \Phi_{M,\,p} w_{M,\,k}\right).$$

It has been shown (Lowan, 1957) that an upper bound for $w_{h,\,k}$ is $\sqrt{2}$. It is necessary that the stability condition, Equation (A12), hold so that the **A** matrix has the proper form (**A***) in order for the upper bound on the eigenvector components to be valid. Thus

$$C_k^{(p)} = \sqrt{2}\Phi^*$$

where Φ^* is an upper bound of the components of the $\mathbf{\Phi}_p$'s.

Equation (A19) now yields

$$d_h^{m+1} < 2M\,(m+1)\,\Phi^*. \tag{A20}$$

Thus by Equation (A14), it can be seen that as Δt and $\Delta r \to 0$, $d_h^{m+1} \to 0$ provided that the stability condition, Equation (A12), is satisfied. Furthermore, the finite-difference scheme is second-order accurate in the time step and third-order accurate in the spatial step.

Acknowledgements

We thank J. F. Hays, J. A. Wood, and R. T. Reynolds for copies of their papers before publication. One of us (Solomon) was a Postdoctoral Fellow of the National Science Foundation during the period of this work. Research was supported by NASA Grant NGL 22–009–187.

References

Anderson, D. L. and Phinney, R. A.: 1967, 'Early Thermal History of the Terrestrial Planets', in *Mantles of the Earth and Terrestrial Planets*, (ed. by S. K. Runcorn), Interscience, p. 113.
Baldwin, R. B.: 1971, *Phys. Earth Planetary Int.* **4**, 167.
Cohen, L. H., Ito, K., and Kennedy, G. C.: 1967, *Am. J. Sci.* **265**, 475.
Cremers, C. J.: 1971, *AIAA J.*, in press.
Duke, M. B. and Silver, L. T.: 1967, *Geochim. Cosmochim. Acta* **31**, 1637.
Dyal, P. and Parkin, C. W.: 1971, *Geochim. Cosmochim. Acta, Suppl.* **2**, 2391.
Fish, R. A., Goles, G. G., and Anders, E.: 1960, *Astrophys. J.* **132**, 243.
Fleischer, R. L., Price, P. B., and Walker, R. M.: 1965, *J. Geophys. Res.* **70**, 2703.

Fricker, P. E., Reynolds, R. T., and Summers, A. L.: 1967, *J. Geophys. Res.* **72**,49. 26
Goetze, C. and Brace, W. F.: 1971, *Tectonophysics*, in press.
Hanks, T. C. and Anderson, D. L.: 1969, *Phys. Earth Planetary Int.* **2**, 19.
Hays, J. F.: 1971, *Phys. Earth Planetary Int.* **5**, 77.
Hohenberg, C. M., Munk, M. N., and Reynolds, J. H.: 1967, *J. Geophys. Res.* **72**, 3139.
Horai, K., Simmons, G., Kanamori, H., and Wones, D.: 1970, *Geochim. Cosmochim. Acta, Suppl.* **1**, 2243.
Husain, L., Schaeffer, O. A., and Sutter, J. F.: 1972, *Science* **175**, 428.
Kopal, Z.: 1962, *Planetary Space Sci.* **9**, 625.
Lachenbruch, A. H.: 1968, *J. Geophys. Res.* **73**, 6977.
Langseth, M. E., Clark, S. P., Jr., and Wexler, A.: 1971, 'The Apollo 15 Lunar Heat Flow Measurement', paper presented at the Lunar Science Institute Conference on Lunar Geophysics, Houston, Texas.
Latham, G., Ewing, M., Dorman, J., Lammlein, D., Press, F., Toksöz, N., Sutton, G., Dunnebier, F., and Nakamura, Y.: 1971, *Science* **174**, 687.
Levin, B. J.: 1962, 'Thermal History of the Moon', in *The Moon*, (ed. by Z. Kopal and Z. K. Mikhailov), Academic Press, New York, p. 157.
Lowan, A. N.: 1957, *The Operator Approach to Problems of Stability and Convergence of Solutions of Difference Equations and the Convergence of Various Iteration Procedures, Scripta Mathematica,* Yeshiva University, New York.
LSPET (Lunar Sample Preliminary Examination Team): 1969, *Science* **165**, 1211.
LSPET (Lunar Sample Preliminary Examination Team): 1972, *Science* **175**, 363.
MacDonald, G. J. F.: 1959, *J. Geophys. Res.* **64**, 1967.
MacDonald, G. J. F.: 1963, *Rev. Geophys.* **1**, 587.
Mason, B. and Melson, W. G.: 1970, *The Lunar Rocks*, Wiley Interscience, New York.
McConnell, R. K., Jr., McClaine, L. A., Lee, D. W., Aronson, J. R., and Allen, R. V.: 1967, *Rev. Geophys.* **5**, 121.
Murase, T. and McBirney, A. R.: 1970, *Science* **170**, 165.
O'Keefe, J. A.: 1970, *EOS, Trans. Am. Geophys. Union* **51**, 633.
Orowan, E.: 1965, *Phil. Trans. Roy. Soc. London, Ser. A,* **258**, 284.
Papanastassiou, D. A. and Wasserburg, G. J.: 1971, *Earth Planetary Sci. Letters* **11**, 37.
Reynolds, R. T., Fricker, P. E., and Summers, A. L.: 1966, *J. Geophys. Res.* **71**, 573.
Reynolds, R. T., Fricker, P. E., and Summers, A. L.: 1971, 'Thermal History of the Moon', to be published.
Ringwood, A. E.: 1970, *J. Geophys. Res.* **75**, 6453.
Ringwood, A. E. and Essene, E.: 1970, *Geochim. Cosmochim. Acta, Suppl.* **1**, 769.
Runcorn, S. K.: 1962, *Nature* **195**, 1150.
Schatz, J. F.: 1971, 'Thermal Conductivity of Earth Materials at High Temperatures', Ph.D. thesis, Massachusetts Institute of Technology, Cambridge.
Sill, W. R.: 1971, *J. Geophys. Res.* **76**, 251.
Singer, S. F.: 1970, *EOS, Trans. Am. Geophys. Union* **51**, 637.
Sonett, C. P., Colburn, D. S., Dyal, P., Parkin, C. W., Smith, B. F., Schubert, G., and Schwartz, K.: 1971, *Nature* **230**, 359.
Sonett, C. P., Colburn, D. S., and Schwartz, K.: 1968, *Nature* **219**, 924.
Ter Haar, G. L.: 1948, *Kgl. Danske Videnskip. Selskab., Mat.-Fys. Medd.* **25**, 3.
Tozer, D. C.: 1970, *Phys. Earth Planetary Int.* **2**, 393.
Tozer, D. C.: 1971, 'An Interpretation of the Lunar Electrical Conductivity Distribution', paper presented at the Lunar Science Institute Conference of Lunar Geophysics, Houston, Texas.
Turcotte, D. L. and Oxburgh, E. R.: 1969a, *J. Geophys. Res.* **74**, 1458.
Turcotte, D. L. and Oxburgh, E. R.: 1969b, *Nature* **223**, 250.
Urey, H. C.: 1952, *The Planets, Their Origin and Development*, Yale University Press, New Haven, Connecticut.
Urey, H. C.: 1968, *Science* **162**, 1408.
Weertman, J.: 1970, *Rev. Geophys. Space Phys.* **8**, 145.
Wood, J. A.: 1971, 'Thermal History and Early Magmatism in the Moon', in *The Geophysical Interpretation of the Moon* (ed. by G. Simmons), in press.
Wood, J. A., Dickey, J. S., Jr., Marvin, U. B., and Powell, B. N.: 1970, *Science* **167**, 602.